



Geophysical Research Letters

RESEARCH LETTER

10.1029/2021GL097019

Key Points:

- Events of an additional ionospheric (F3) layer are first reported at Arecibo
- The formation of the F3 layers is mainly due to the gradient of the vertical ion drift
- The height variation of the vertical ion drift is largely due to the zonal electric field

Correspondence to:

Y. Gong and S. Zhang, yun.gong@whu.edu.cn; zsd@whu.edu.cn

Citation:

Gong, Y., Lv, X., Zhang, S., Zhou, Q., & Ma, Z. (2022). The first observation of additional ionospheric layers over Arecibo using an incoherent scatter radar. *Geophysical Research Letters*, 49, e2021GL097019. https://doi.org/10.1029/2021GL097019

Received 11 NOV 2021 Accepted 22 FEB 2022

The First Observation of Additional Ionospheric Layers Over Arecibo Using an Incoherent Scatter Radar

Yun Gong^{1,2}, Xiedong Lv^{1,2}, Shaodong Zhang^{1,2,3}, Qihou Zhou⁴, and Zheng Ma^{1,2}

¹School of Electronic Information, Wuhan University, Wuhan, China, ²Key Laboratory of Geospace Environment and Geodesy, Ministry of Education, Wuhan, China, ³State Key Laboratory of Information Engineering in Surveying, Mapping and Remote Sensing, Wuhan University, Wuhan, China, ⁴Electrical and Computer Engineering Department, Miami University, Oxford, OH, USA

Abstract We present an analysis of additional ionospheric F-region layers, the F3 layers at Arecibo (18.3°N, 32°N geomagnetic latitude). The F3 layer is often observed in low geomagnetic latitudes observed above the F2 layer. This is the first time that the F3 layer is reported at Arecibo, which has a dip angle of 43.6°. Three F3 layer events were captured by the Arecibo incoherent scatter radar at around 400 km in the period of 03:00–07:00 LT, 04:00–06:00 LT, and 02:00–06:30 LT on 30 November, 1 December, and 2 December 2016, respectively. The formation of the observed layers is largely due to the change of the height gradient of the vertical ion drift, which accumulates the electrons at around 400 km. This generation mechanism is further verified by the simulation. The altitudinal variation of the vertical ion drift is mainly due to the effect of the westward electric field.

Plain Language Summary In the low geomagnetic latitudes of +/-15°, an additional ionospheric layer above the ionospheric F2 peak is often observed. The additional layer, often called F3 layer, is suggested to be generated by the upward ion drift over the F2 peak. Using incoherent scatter radar (ISR) measurements at Arecibo (18.3°N, 32°N geomagnetic latitude), Puerto Rico, we provide the first observations of F3 layer events at geomagnetic mid-latitudes. Three events of the F3 layer were captured by the Arecibo ISR at around 400 km in the period of 03:00–07:00 LT, 04:00–06:00 LT, and 02:00–06:30 LT on 30 November, 1 December, and 2 December 2016, respectively. Our analysis shows that the observed F3 layers were formed due to the change in the height gradient of the downward vertical ion drifts that result in a large plasma influx at about 400 km. The vertical variation of the downward vertical ion drift is largely due to the effect of the westward electric field. Our results provide a good example that the F3 layer could be formed largely due to the vertical transport at the geomagnetic mid-latitude, which improves our understanding of the F3 layer.

1. Introduction

The F3 layer, an additional ionospheric F-region layer above the normal F2 layer has been observed since the 1940s using ground-based ionosonde measurements (e.g., Ratcliffe, 1951; Sen, 1949; Skinner et al., 1954). In 1995, Balan and Bailey (1995) investigated the structure of stratification above the F2 layer as a mechanism for the F3 layer using the Sheffield University Plasmasphere Ionosphere model (SUPIM). Since then, the F3 layer has been studied extensively both theoretically and observationally (e.g., Balan et al., 1997, 1998; Batista et al., 2002; Chaitanya et al., 2013, 2016; Fagundes et al., 2011; Hsiao et al., 2001; Jenkins et al., 1997; Klimenko & Klimenko, 2012; Klimenko et al., 2011, 2012; Lynn et al., 2000; Mridula & Pant, 2018; Rama Rao et al., 2005; Sreeja et al., 2010; Tardelli et al., 2016; Uemoto et al., 2007; Venkatesh et al., 2019, 2020; Zain et al., 2008; Zhao, Wan, Reinisch et al., 2011; Zhao, Wan, Yue, et al., 2011; Zhao et al., 2014). Applying the SUPIM model, Balan et al. (1998) suggested that the F3 layer is likely due to the upward $E \times B$ drift with the meridional neutral wind playing a minor role. Using measurements from oblique and vertical ionosondes, Lynn et al. (2000) presented the first observational study on the latitudinal variation of the F3 layer at equatorial latitudes in Southeast Asia. They found that the F3 layer primarily occurred in a latitudinal range from 4° to 18° on the southern side of the magnetic equator. Applying long-term observational data at Fortaleza in Brazil, Batista et al. (2002) reported that the additional layer more likely appeared during the local summer and winter than the equinoxes. Rama Rao et al. (2005) found that the occurrence of the F3 layer decreases with increasing solar activity. The F3 layer is predicted to form during the morning-noon period (Balan et al., 1998), but the time of occurrence can extend to afternoon (14:00–16:00 LT) during the storm time (Balan et al., 2008; Klimenko et al., 2011) or even post-sunset

© 2022. American Geophysical Union. All Rights Reserved.

GONG ET AL.



(18:00-21:00 LT) (Zhao, Wan, Reinisch, et al., 2011). Using the Global Self-Consistent Model of the Thermosphere, Ionosphere, and Protonosphere, Klimenko and Klimenko (2012) investigated the formation mechanisms of the F3 layer. They stated that the height varying vertical plasma drift is important in forming the F3 at the equatorial region. Zhao et al. (2014) presented statistical results of the global characteristics of the F3 layer based on the observation made by the Constellation Observing System for Meteorology, Ionosphere and Climate satellite between April 2006 and August 2014. Their results show that the F3 layer most frequently occurs in the geomagnetic latitudinal range of ±15° and the time of occurrence is largely after 08:00 LT. Mridula and Pant (2018) investigated the occurrence of the post-noon F3 layer over dip equatorial station Thiruvananthapuram in India. They found that the reversal of the E region electric field plays a crucial role in the generation of the afternoon F3 layers. Venkatesh et al. (2019) reported an F3 layer occurred over a large latitudinal extent from 20°S to 25°N dip latitudes during a storm that occurred on 17 March 2015. The F3 layer is proposed to be related to prompt penetration electric field (PPEF) phases. Using the Jicamarca (1.9°S, 282.7°E, 0.5°S magnetic latitude) incoherent scatter radar (ISR) measurements from 2014 to 2018, Venkatesh et al. (2020) presented a systematic observation of an F3 layer at equatorial region. Their study suggested that the F3 layer observed at Jicamarca is less prominent than those of other low latitudes. According to the previous studies, the F3 layer is generally recognized as an equatorial ionospheric phenomenon and its occurrence depends on magnetic and solar activities. A review of the studies on the F3 layer in the low latitude ionosphere can be found in Balan et al. (2018) and references therein.

In this study, we investigate the structure and the formation mechanism of the F3 layers observed at Arecibo, Puerto Rico (18.3°N, 66.7°W, 32°N geomagnetic latitude). To our knowledge, this is the first time that F3 layers have been reported at Arecibo, a station at mid-geomagnetic latitude, despite over 50 years of operation. Data processing methods are described in Section 2. Results and discussions are presented in Section 3 and conclusions are summarized in Section 4.

2. Data Description

The experiment was conducted at Arecibo Observatory using the dual-beam ISR in the period from 30 November to 2 December 2016. The Linefeed was pointed at the zenith all the time while the Gregorian feed rotated at a fixed 15° zenith angle during the observation. The observation used the coded long-pulse technique described by Sulzer (1986). This study uses line-of-sight (LOS) ion drifts, electron density, electron and ion temperature, all of which are directly obtained by processing the ISR power spectrum. The altitudinal resolution of these ionospheric parameters is 12 km. Vector ion drifts in the directions of anti-parallel to the geomagnetic field (ν_{ap} , positive is upward in the anti-parallel direction of geomagnetic field line) and perpendicular to $\bf{\it B}$ and northward (ν_{pn} , positive is in the direction of upward and northward) are converted from the LOS ion drifts using the linear regularization method described by Sulzer et al. (2005). Note that the derivation of the vector ion drifts using the Arecibo ISR depends on the measurements from the Gregorian feed because only the Gregorian feed was rotated through the experiment to collect LOS ion drifts at different directions (e.g., Gong & Zhou, 2011; Sulzer et al., 2005). However, the data obtained from the Gregorian feed above 420 km is not available and consequently, the vector ion drifts (ν_{pn} and ν_{ap}) are limited below 420 km. The data measured from the Linefeed is available up to 1,000 km.

In the geomagnetic coordinate, the vertical ion motion (v_z , positive is upward) consists of v_{nn} and v_{nn} via,

$$v_z = v_{\rm pn} \cos I + v_{\rm ap} \sin I \tag{1}$$

where I denotes the dip angle. At Arecibo, I is 43.6° , which means that $v_{\rm pn}$ and $v_{\rm ap}$ almost have the same weight on v_z . The anti-parallel ion drift is associated with the diffusion velocity (v_d) and meridional wind (u_s) via (e.g., Gong et al., 2012),

$$v_{\rm ap} = u_s \cos I + v_d \tag{2}$$

where v_d depends on electron concentration, electron and ion temperature, and most importantly ambipolar diffusion coefficient. A detailed derivation of v_d can be found in Gong et al. (2012). However, the derivation of the meridional wind using the Arecibo ISR is not very accurate above 350 km, because any inaccuracy in measurements is greatly amplified due to the very large ambipolar diffusion coefficient at that region (Gong &

GONG ET AL. 2 of 8

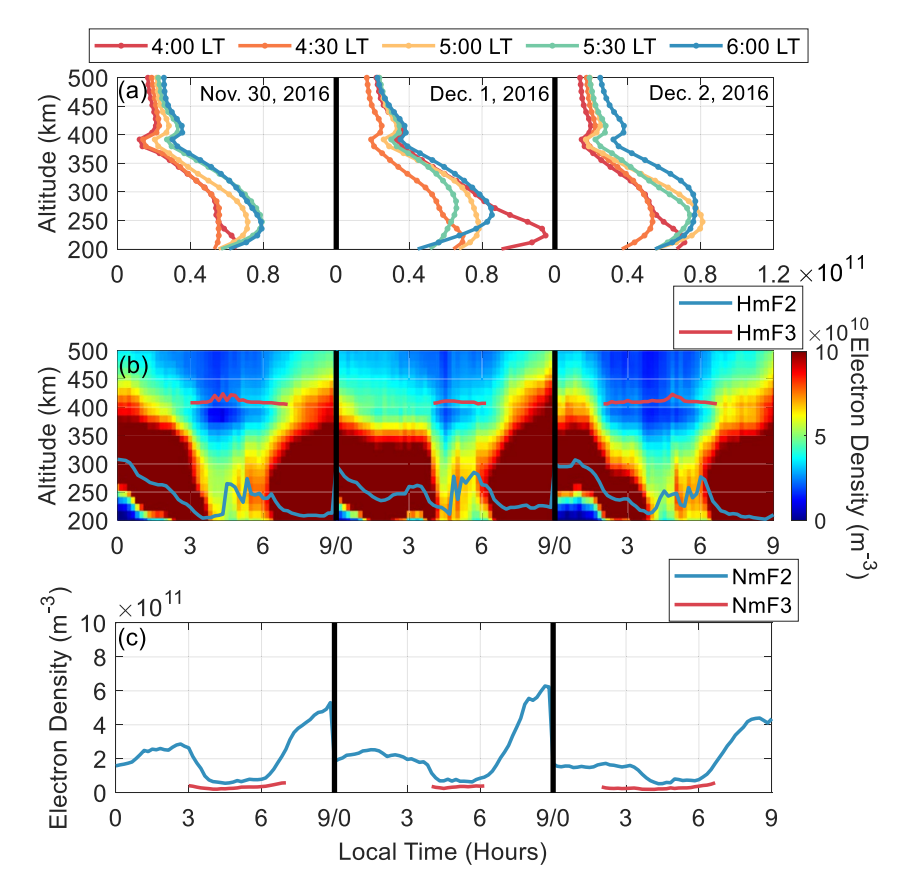


Figure 1. (a) Vertical distribution of electron density in the altitude range from 200 to 500 km at 04:00 LT (red), 04:30 LT (orange), 05:00 LT (yellow), 05:30 LT (green), and 06:00 LT (blue) on 30 November (left), 1 December (middle), and 2 December 2016 (right); (b) height-and-time electron density distribution, and ionospheric peak heights (HmF2, blue curve; HmF3, red curve) from 00:00 LT to 09:00 LT on 30 November (left), 1 December (middle), and 2 December 2016 (right); (c) temporal variations of the peak concentrations (NmF2, blue curve; NmF3, red curve), respectively on 30 November (left), 1 December (middle), and 2 December 2016 (right).

Zhou, 2011). In this study, we use v_{ap} instead of u_s to avoid the uncertainties. A more detailed description of ISR measurement techniques can be found in Zhou and Sulzer (1997).

3. Results and Discussion

Figure 1a presents the vertical distribution of electron density in an altitude range from 200 to 500 km at 04:00 LT (red), 04:30 LT (orange), 05:00 LT (yellow), 05:30 LT (green), and 06:00 LT (blue) on 30 November (left), 1 December (middle), and 2 December 2016 (right). As seen from Figure 1a, in the three consecutive days, an additional peak over the ionospheric F2 peak is observed at ~400 km. A method that estimates the relative error of the electron density obtained from Arecibo ISR is described in Zhou et al. (1995). Based on the method, the relative error of the electron density is less than 4% at 400 km. In order to better locate the F3 peak, the electron density profile is interpolated to have a 1 km height resolution. Figures 1b and 1c show the temporal variations of the ionospheric peak heights (HmF2, blue curve; HmF3, red curve) and peak concentration (NmF2, blue curve; NmF3, red curve), respectively.

According to Figure 1b, the F3 layers commenced at ~03:00 LT on 30 November, ~04:00 LT on 1 December, and ~02:00 LT on 2 December. The F3 peak lasted for 4 hr on 30 November, 2 hr on 1 December, and 4.5 hr on 2 December. When the F3 peaks exist, the HmF2 is in an altitude range from 200 to 300 km. The HmF2 shows the typical nighttime variation at Arecibo. A rapid drop of HmF2, the so-called midnight collapse, occurred around midnight which is a prominent and common ionospheric feature at Arecibo (Gong et al., 2012). In the period from ~03:00 LT to ~06:00 LT, the NmF2 which is shown in Figure 1c is about two times larger than the NmF3.

GONG ET AL. 3 of 8

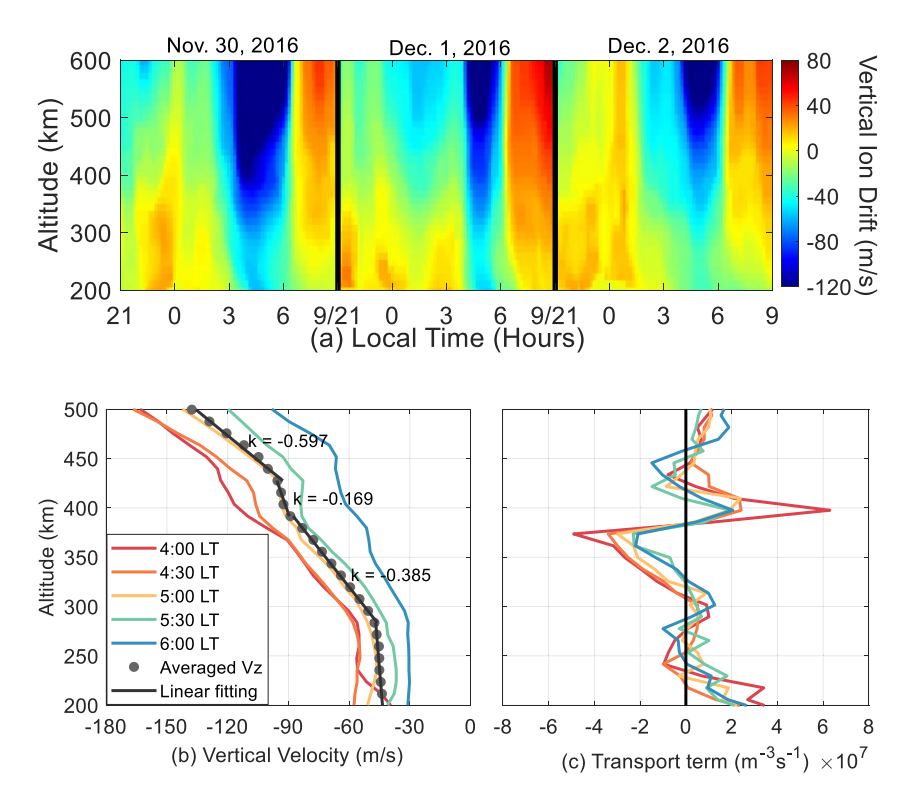


Figure 2. (a) Range-time-intensity plots of the vertical ion drift (positive upward) in the period from 00:00 LT to 09:00 LT, respectively on November 30 (left), December 1 (middle) and December 2 (right), 2016; (b) vertical variation of the vertical velocity (v_z) at 04:00 LT (red), 04:30 LT (orange), 05:00 LT (yellow), 05:30 LT (green), 06:00 LT (blue), the averaged v_z in the period from 04:00 LT to 06:00 LT (black dots) and its linear fitting (black lines) on 30 November 2016, k represents the height gradient of v_z ; (c) vertical variation of the transport term ($-\nabla \cdot (N_e \cdot v_z)$) at 04:00 LT (red), 04:30 LT (orange), 05:00 LT (yellow), 05:30 LT (green) and 06:00 LT (blue) on 30 November 2016.

According to previous studies, the F3 layer most likely occurs after 08:00 LT (e.g., Rama Rao et al., 2005) and it is considered as a phenomenon within $\pm 15^{\circ}$ of the geomagnetic latitudes (e.g., Zhao et al., 2014). This makes our observation very interesting since the F3 layers are observed during nighttime and the geomagnetic latitude of Arecibo is $\sim 32^{\circ}$ N.

Since the ion production rate during the night is very low and the recombination rate is slow at ~400 km, the formation of the F3 peak is very likely due to the vertical transport. Figure 2a shows the temporal variations of the vertical ion drift in the altitude range of 200-600 km from 00:00 LT to 09:00 LT on 30 November, 1 December, and 2 December respectively. As shown in Figure 2a, the vertical ion drift is largely downward during the night, which is typical at Arecibo. The downward ion drift from 03:30 LT to 6:00 LT is particularly prominent. This indicates that the large topside flux transports ions downward, which may help in the formation of the F3 layer. However, since a constant ion drift can only push the F2 layer up or down, the F3 layer cannot be generated. The topside flux could not play a direct role in the formation of the F3 layer. In order to better reveal the altitudinal structure of the vertical ion drift, Figure 2b presents the vertical ion drift in the altitude range from 200 to 500 km at 04:00 LT (red), 04:30 LT (orange), 05:00 LT (yellow), 05:30 LT (green), and 06:00 LT (blue) on 30 November 2016. The black dots are the averaged vertical ion drift in the period from 04:00 LT to 06:00 LT on 30 November 2016. As seen from Figure 2b, the magnitude of the vertical ion drift largely decreases with decreasing altitude but with different gradients (k = dv / dh) in different regions. As shown by the black dots in Figure 2b, in the altitude range from 500 to 430 km, the magnitude of the downward ion drift quickly decreases from 140 m/s to 95 m/s with a gradient of -0.597×10^3 s. From 430 to 400 km, the magnitude of the downward ion drift changes slowly and the gradient is -0.169×10^3 s. From 400 to 300 km, the magnitude of the vertical ion drift rapidly decreases again from 90 m/s to 45 m/s and the gradient is -0.385×10^3 s. The altitudinal variation of the gradient of v_z may establish the condition for the ions to be accumulated at around 400 km.

GONG ET AL. 4 of 8



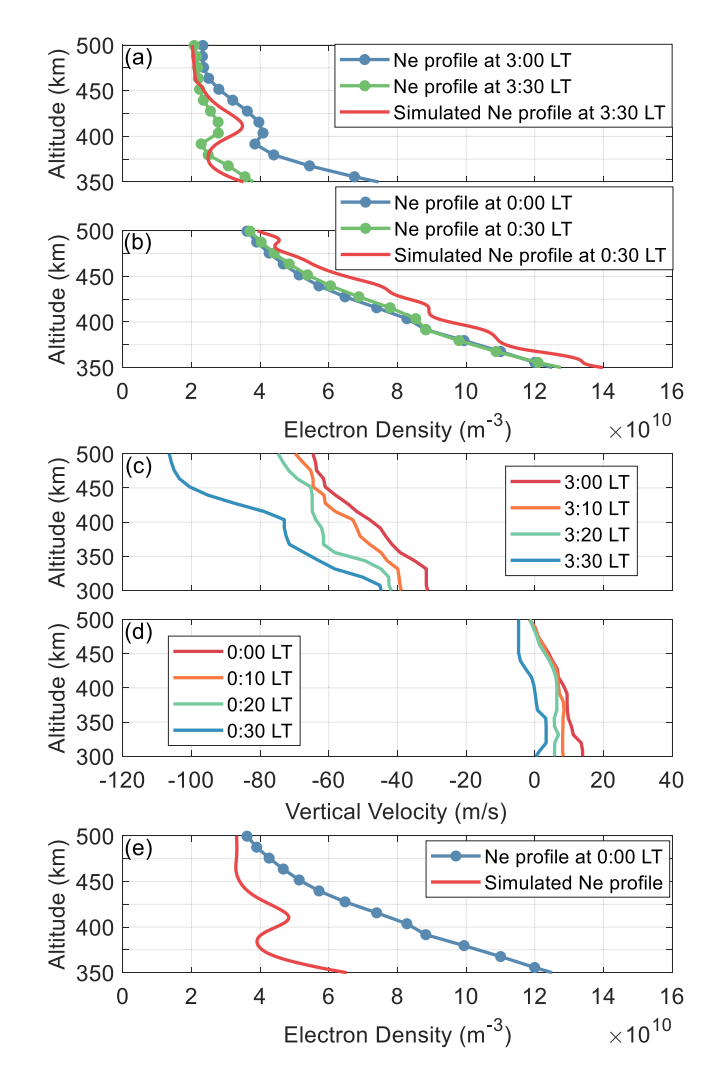


Figure 3. (a) Vertical variation of the electron density at 3:00 LT (blue) and 3:30 LT (green) 30 November 2016, and simulated electron density profile at 3:30 LT (red) 30 November 2016; (b) the same as (a) but for the time instant at 0:00 LT (blue, observed), 0:30 LT (green, observed), and 0:30 LT (red, simulated) 30 November 2016. (c) vertical variation of the vertical ion drift (v_z) at 3:00 LT (red), 3:10 LT (orange), 3:20 LT (green) and 3:30 LT (blue); (d) the same as (c) but for the time instant at 0:00 LT (red), 0:10 LT (orange), 0:20 LT (green) and 0:30 LT (blue) 30 November 2016; (e) initial vertical profile of the electron density at 0:00 LT (blue) 30 November 2016, and simulated electron density profiles with v_z in the period of 3:00–3:30 LT (red) 30 November 2016.

The time-dependent continuity equation can be written as (e.g., Rishbeth, 1986; Liu et al., 2013):

$$\frac{\partial N_e}{\partial t} = P - L - \nabla \cdot \left(N_e \overrightarrow{V} \right) = P - \beta N_e - \nabla \cdot \left(N_e \overrightarrow{V} \right) \tag{3}$$

where N_e is the electron density, P is the production rate, L is the loss rate, \overrightarrow{V} is the plasma velocity. The recombination coefficient of O^+ , β , is calculated via (Schunk & Nagy, 2009) $\beta = 3.7 \times 10^{-12} (250/Te)^{0.7} \text{ cm}^3 \text{s}^{-1}$, where Te is the electron temperature. The horizontal gradients of N_e and \vec{V} are much smaller than those in the vertical direction and thus have a limited contribution to the transport term of the equation. Since the production rate is very low during the nighttime and the recombination rate is slow above the F2 peak, the nighttime vertical electron distribution depends mainly on the transport term $-\nabla \cdot (N_a \cdot v_a)$. The vertical variation of the transport term at 04:00 LT (red), 04:30 LT (orange), 05:00 LT (yellow), 05:30 LT (green), and 06:00 LT (blue) on 1 December 2016 is presented in Figure 2c. As seen from Figure 2c, the transport term is positive at around 400 km, which indicates that electrons accumulate over time at this altitude. At around 380 km, the transport term is negative, indicating that a dip is expected at this height. The combination of a convergence at 400 km and a depletion at 380 km produces a prominent F3 layer.

To further understand our observation, numerical simulations using the time-dependent continuity equation mentioned above are presented. Two observation periods, 03:00-03:30 LT and 0:00-0:30 LT 30 November, are selected to represent the double-peak period and the non-double-peak period respectively. The vertical profiles of N_e at 03:00 LT 30 November and 0:00 LT 30 November are used as the initial condition for the doublepeak and the non-double-peak periods, respectively. The observational data of electron density at 00:00 LT and 3:00 LT 30 November and vertical ion drift are interpolated in height and time respectively to have 1 km and 1 s altitudinal and temporal resolutions. The upper and lower boundaries are set to 600 and 250 km, respectively. We averaged the electron density at 600 and 250 km during the double-peak and non-double-peak periods, respectively. Then, we set the average as the boundary condition for electron density. The temporal variation of electron density with the effects of the transport term $-\nabla \cdot (N_e \vec{V})$ and the recombination term $-\beta N_e$ are simulated using Equation 3. The simulation results of the double-peak and the non-double-peak periods are presented in Figures 3a and 3b, respectively. Figure 3a presents the vertical variation of the electron density at 3:00 LT (blue) and 3:30 LT (green) 30 November 2016, and simulated electron density profile at 3:30 LT (red) 30 November 2016. Figure 3b is the same as Figure 3a but for the time instant at 0:00 LT (blue, observed), 0:30 LT (green, observed), and 0:30 LT

(red, simulated) 30 November 2016. The vertical ion drifts used in the simulation of the double-peak and the non-double-peak periods are presented in Figures 3c and 3d, respectively.

As shown in Figures 3a and 3b, the simulated electron density profile at 3:30 LT 30 November 2016, presents a prominent additional stratification at \sim 400 km while the simulated profile at 0:30 LT 30 November 2016, did not even show a topside ionosphere ledge. The simulated N_e profile at 3:30 LT has a similar trend as the observation (green curve). Although this simulation cannot be a sufficient proof for the vertical ion drift being the only mechanism for the formation of stratification, it demonstrates that the vertical ion drift could play an important role in generating an additional layer at the altitude of \sim 400 km. As seen from Figures 3c and 3d, the height variation of v_z used in the double-peak and the non-double-peak periods are very different. During the non-double-peak period, the vertical variation of v_z is limited. In order to reveal the importance of the vertical variation of v_z , we run another simulation in which v_z in the double-peak period and the initially observed electron density profile at

GONG ET AL. 5 of 8

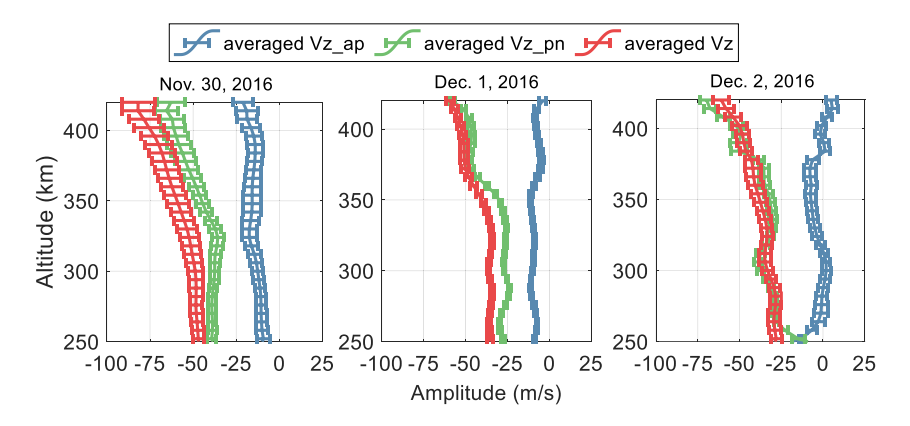


Figure 4. The vertical variations of v_z (red), v_{pn} (green), and v_{ap} (blue) in the altitude range between 250 and 420 km respectively on 30 November (left panel), 1 December (middle panel), and 2 December (right panel), 2016. The results are averaged in the period of 3:00 LT to 7:00 LT on 30 November, 4:00 LT to 6:00 LT on 1 December, and 2:00 LT to 6:30 LT on 2 December. The error bars represent the range of one standard deviation of v_z , $v_{z,pn}$, and $v_{z,ap}$ in the double-peak period at each height.

00:00 LT are applied. As we can see from Figure 3e, if the initial N_e profile is approximate exponential decaying with height and combined with v_e in the double-peak period, the simulation shows that an F3 layer can be formed.

Previous studies (e.g., Balan et al., 1998) suggested that the formation of the F3 peak is due to the upward ion drift over the F2 peak. While the F2 layer was lifted upward and became the F3 layer, a new F2 layer developed at an altitude of the original F2 peak through photochemical processes and dynamics. Since the production of ionization and upward ion drifts are essential for the formation of the F3 layer, this kind of stratification occurs only during daytime and at the equatorial locations where the dip angle is small and $E \times B$ drift is sufficient enough to support the upward drift. Klimenko and Klimenko (2012) stated that during the nighttime, the F3 layer can be formed by the height gradient of the vertical plasma drift caused by the zonal electric field at the geomagnetic equator. However, based on our observation shown in Figures 1 and 2, the additional layers occurred when the drift was downward and the solar ionization rate was low. Besides, Arecibo Observatory is located in the middle geomagnetic latitude. Thus, the conditions for F3 occurrence at Arecibo are quite different from the observations at low latitudes reported by previous studies. Our study presents the first case that the F3 layer is mainly caused by the vertical drift gradient in the geomagnetic mid-latitude.

Based on Figures 1 and 2, the vertical ion drift is key to the formation of the F3 layer. v_z is composed of the projections of $v_{\rm pn}$ and $v_{\rm ap}$ in the vertical direction. $v_{\rm pn}$ is controlled by the zonal electric field via $E \times B$. $v_{\rm ap}$ is associated with the meridional wind and diffusion velocity. At the geomagnetic equator, the effect of meridional wind and diffusion to the vertical ion drift is negligible because the dip angle is zero, while at Arecibo, the dip angle is 43.6°. According to Equation 1, $v_z = 0.72v_{\rm pn} + 0.69v_{\rm ap}$, which indicates that the zonal electric field and meridional wind are both important in controlling the vertical ion drift. To further investigate the variation of v_z in the double-peak period, altitudinal variations of v_z (red), the vertical components due to electric field ($v_{z_{\rm ap}}$, green) and parallel to E drift ($v_{z_{\rm ap}}$, blue) averaged during the periods of the F3 layers on 30 November (left), 1 December (middle), and 2 December 2016 (right) are presented in Figure 4. The standard deviations of v_z , $v_{z_{\rm pn}}$, and $v_{z_{\rm ap}}$ in the double-peak period at each height are also calculated and presented as error bars in Figure 4.

As seen from Figure 4, the vertical variation between v_z and v_{z_pn} are very similar, while the vertical variation of v_{z_ap} is limited. Hence, the formation of the F3 layer is mainly due to the height gradient of the downward ion drift caused by the westward electric field. Gong et al. (2013) reported that the geomagnetic storm could have a large impact on the variation of the zonal electric field at Arecibo. During our observation, the geomagnetic activity is quiet (Kp index is less than 2 and the Dst index is greater than -10 nT), and the solar activity is low (less than 85 solar flux unit (SFU), 1SFU = 10^{-22} W/m²/Hz). Hence, the geomagnetic and solar activities are not responsible for the vertical variation of v_{pn} . The formation of the observed F3 layer is mainly due to the effects of the vertical ion drift gradient, which is consistent with the study reported by Klimenko and Klimenko (2012) for the equatorial ionosphere. In general, the vertical variation of v_{pn} at Arecibo is limited (e.g., Zhou & Sulzer, 1997). Further studies using a substantial data set are needed to investigate the reason why the zonal electric field could have a

GONG ET AL. 6 of 8

7 of 8



Acknowledgments

AGS-2152109

GONG ET AL.

The Arecibo Observatory is operated by

the University of Central Florida under

a cooperative agreement with the U.S.

is supported by the National Natural

Science Foundation of China (through

grants 41574142 and 42104145), and the

U.S. National Science Foundation grant

National Science Foundation. The study

large vertical variation above 300 km. Note that traveling ionospheric disturbances/gravity waves (TIDs/GWs) could be a potential source for the change in vertical transport. However, the study of the effect of TIDs/GWs on the vertical ion motion is beyond the current scope of the paper.

4. Summary and Conclusion

The F3 layer is recognized as a general structure that occurs in the lower geomagnetic latitudes. Using the Arecibo incoherent scatter radar (18.3°N, 32°N geomagnetic latitude) measurements in the periods from 30 November to 2 December 2016, three F3 layer events have been observed. To our knowledge, this is the first time that F3 layers have been reported at Arecibo. The F3 layers commenced on ~03:00 LT 30 November, ~04:00 LT 1 December, and ~02:00 LT 2 December, and lasted for 4, 2, and 4.5 hr, respectively. The F3 layers are at about 400 km and the concurrent F2 peaks are in an altitude range from 200 to 300 km. In the periods of 03:00 LT to 06:00 LT on 30 November, 1 December, and 2 December, significant downward vertical ion drift is observed above 300 km, and the gradient of the downward ion drift is strongly height dependent.

Our analysis reveals that the observed F3 layers are mainly generated by the height variation of the downward ion drift, which is largely caused by the westward electric field. Our simulation verifies that the observed vertical ion drift could play an important role in generating the F3 layer. This study presents a first case that the F3 layer could be formed mainly by the gradient of the vertical transport at the geomagnetic mid-latitude. Nevertheless, more cases need to be studied to better understand the formation mechanism and occurrence of the F3 layer at Arecibo.

Data Availability Statement

The Arecibo data used here can be obtained from the Madrigal Database at the Arecibo Observatory through http://www.naic.edu/madrigal/index.html/. The geomagnetic and solar activities indices Kp, Dst, and F_{10.7} can be downloaded from the SPDF OmniWeb database (https://omniweb.gsfc.nasa.gov/form/dx1.html).

References

Balan, N., & Bailey, G. J. (1995). Equatorial plasma fountain and its effects: Possibility of an additional layer. *Journal of Geophysical Research*, 100, 21421–21432. https://doi.org/10.1029/95JA01555

Balan, N., Bailey, G. J., Abdu, M. A., Oyama, K. I., Richards, P. G., Macdougall, J., & Batista, I. S. (1997). Equatorial plasma fountain and its effects over three locations: Evidence for an additional layer, the F3 layer. *Journal of Geophysical Research*, 102, 2047–2056. https://doi.org/10.1029/95JA02639

Balan, N., Batista, I. S., Abdu, M. A., Macdougall, J., & Bailey, G. J. (1998). Physical mechanism and statistics of occurrence of an additional layer in the equatorial ionosphere. *Journal of Geophysical Research*, 103, 29169–29181. https://doi.org/10.1029/98JA02823

Balan, N., Li, Q., Liu, L., & Le, H. (2018). An introduction to equatorial electrodynamics and a review of an additional layer at low latitudes. Journal of Atmospheric and Solar-Terrestrial Physics, 181, 94–109. https://doi.org/10.1016/j.jastp.2018.10.011

Balan, N., Thampi, S. V., Lynn, K., Otsuka, Y., Alleyne, H., Watanabe, S., et al. (2008). F3 layer during penetration electric field. *Journal of Geophysical Research*, 113, A00A07. https://doi.org/10.1029/2008JA013206

Batista, I. S., Abdu, M. A., McDougall, J., & Souza, J. R. (2002). Long term trends in the frequency of occurrence of the F3 layer over Fortaleza. Journal of Atmospheric and Solar-Terrestrial Physics, 64, 1409–1412. https://doi.org/10.1016/s1364-6826(02)00104-9

Chaitanya, P. P., Patra, A. K., Balan, N., & Rao, S. V. B. (2013). First simultaneous observations of F3 layer and $E \times B$ drift in Indian sector and modeling. *Journal of Geophysical Research: Space Physics*, 118, 3527–3539. https://doi.org/10.1002/jgra.50298

Chaitanya, P. P., Patra, A. K., Balan, N., & Rao, S. V. B. (2016). Unusual behavior of the low-latitude ionosphere in the Indian sector during the deep solar minimum in 2009. *Journal of Geophysical Research: Space Physics*, 121, 6830–6843. https://doi.org/10.1002/2015ja022061

Fagundes, P. R., Klausner, V., Bittencourt, J. A., Sahai, Y., & Abalde, J. R. (2011). Seasonal and solar cycle dependence of F3-layer near the southern crest of the equatorial ionospheric anomaly. *Advances in Space Research*, 48(3), 472–477. https://doi.org/10.1016/j.asr.2011.04.003

Gong, Y., & Zhou, Q. (2011). Incoherent scatter radar study of the terdiurnal tide in the E- and F-region heights at Arecibo. *Geophysical Research Letters*, 38, L15101. https://doi.org/10.1029/2011GL048318

Gong, Y., Zhou, Q., Zhang, S., Aponte, N., Sulzer, M., & Gonzalez, S. (2012). Midnight ionosphere collapse at Arecibo and its relationship to the neutral wind, electric field, and ambipolar diffusion. *Journal of Geophysical Research*, 117, A08332. https://doi.org/10.1029/2012JA017530

Gong, Y., Zhou, Q., Zhang, S. D., Aponte, N., Sulzer, M., & González, S. A. (2013). The Fregion and topside ionosphere response to a strong geomagnetic storm at Arecibo. *Journal of Geophysical Research: Space Physics*, 118(8), 5177–5183. https://doi.org/10.1002/jgra.50502
 Hsiao, C. C., Liu, J. Y., Tsunoda, R. T., Fukao, S., Saroso, S., Nozaki, K., et al. (2001). Evidence for the geographic control of additional layer

formation in the low latitude ionosphere. *Advances in Space Research*, 27, 1293–1297. https://doi.org/10.1016/s0273-1177(01)00206-x
Jenkins, B., Bailey, G. J., Abdu, M. A., Batista, I. S., & Balan, N. (1997). Observations and model calculations of an additional layer in the topside

Jenkins, B., Bailey, G. J., Abdu, M. A., Batista, I. S., & Balan, N. (1997). Observations and model calculations of an additional layer in the topside ionosphere above Fortaleza, Brazil. *Advances in Space Research*, 15, 753–759. https://doi.org/10.1007/s00585-997-0753-3

Klimenko, M. V., & Klimenko, V. V. (2012). Mechanisms of stratification of the F2 layer and formation of the F3 and G layers in the equatorial ionosphere. *Geomagnetism and Aeronomy*, 52(3), 321–334. https://doi.org/10.1134/s0016793212030097

Klimenko, M. V., Klimenko, V. V., & Karpachev, A. T. (2012). Formation mechanism of additional layers above regular F2 layer in the near-equatorial ionosphere during quiet period. *Journal of Atmospheric and Solar-Terrestrial Physics*, 90, 179–185. https://doi.org/10.1016/j.jastp.2012.02.011



- Klimenko, M. V., Klimenko, V. V., Ratovsky, K. G., & Goncharenko, L. P. (2011). Disturbances in the ionospheric F-region peak heights in the American longitudinal sector during geomagnetic storms of September 2005. Advances in Space Research, 48(7), 1184–1195. https://doi. org/10.1016/j.asr.2011.06.002
- Liu, L., Chen, Y., Le, H., Ning, B., Wan, W., Liu, J., & Hu, L. (2013). A case study of postmidnight enhancement in F-layer electron density over Sanya of China. *Journal of Geophysical Research: Space Physics*, 118(7), 4640–4648. https://doi.org/10.1002/jgra.50422
- Lynn, K. J. W., Harris, T. J., & Sjarifudin, M. (2000). Stratification of the F2 layer observed over Southeast Asia. *Journal of Geophysical Research*, 105, 27147–27156. https://doi.org/10.1029/2000JA900056
- Mridula, N., & Pant, T. K. (2018). The generation of post noon F3 layers over the dip equatorial location of Thiruvananthapuram-A new perspective. Journal of Atmospheric and Solar-Terrestrial Physics, 170, 55–63. https://doi.org/10.1016/j.jastp.2018.02.008
- Rama Rao, P. V. S., Niranjan, K., Prasad, D. S. V. V. D., Brahmanandam, P. S., & Gopikrishna, S. (2005). Features of additional stratification in ionospheric F2 layer observed for half a solar cycle over Indian low latitudes. *Journal of Geophysical Research*, 110, A04307. https://doi. org/10.1029/2004JA010646
- Ratcliffe, J. A. (1951). Some regularities in the F2 region of the ionosphere. *Journal of Geophysical Research*, 56, 487–507. https://doi.org/10.1029/JZ056j004p00487
- Rishbeth, H. (1986). On the F2-layer continuity equation. Journal of Atmospheric and Solar-Terrestrial Physics, 48(6), 511–519. https://doi.org/10.1016/0021-9169(86)90085-1
- Schunk, R., & Nagy, A. (2009). Ionospheres: Physics, plasma physics, and chemistry. Cambridge university press.
- Sen, H. Y. (1949). Stratification of the F2 layer of the ionosphere over Singapore. Journal of Geophysical Research, 54, 363–366. https://doi.org/10.1029/JZ054i004p00363
- Skinner, N. J., Brown, R. A., & Wright, R. W. (1954). Multiple stratification of the F layer at Ibadan. *Journal of Atmospheric and Solar-Terrestrial Physics*, 5, 92–100. https://doi.org/10.1016/0021-9169(54)90013-6
- Sreeja, V., Ravindran, S., & Pant, T. K. (2010). Features of the F3 layer occurrence over the equatorial location of Trivandrum. Advances in Space Research, 28, 1741–1747. https://doi.org/10.5194/angeo-28-1741-2010
- Sulzer, M. P. (1986). A radar technique for high range resolution incoherent scatter autocorrelation function measurements utilizing the full average power of klystron radars. *Radio Science*, 21, 1033–1040. https://doi.org/10.1029/rs021i006p01033
- Sulzer, M. P., Aponte, N., & Gonzalez, S. A. (2005). Application of linear regularization methods to Arecibo vector velocities. *Journal of Geophysical Research*, 110, A10305. https://doi.org/10.1029/2005JA011042
- Tardelli, A., Fagundes, P. R., Pezzopane, M., Venkatesh, K., & Pillat, V. G. (2016). Seasonal and solar activity variations of F3 layer and quadruple stratification (StF-4) near the equatorial region. *Journal of Geophysical Research: Space Physics*, 121(12), 12–116. https://doi.org/10.1002/2016ia023580
- Uemoto, J., Ono, T., Maruyama, T., Saito, S., Iizima, M., & Kumamoto, A. (2007). Magnetic conjugate observation of the F3 layer using the SEALION ionosonde network. Geophysical Research Letters. 34, L02110. https://doi.org/10.1029/2006GL028783
- Venkatesh, K., Patra, A. K., Balan, N., Fagundes, P. R., Tulasi Ram, S., Batista, I. S., & Reinisch, B. W. (2019). Superfountain effect linked with 17 March 2015 geomagnetic storm manifesting distinct F3 layer. *Journal of Geophysical Research: Space Physics*, 124(7), 6127–6137. https://doi.org/10.1029/2019ja026721
- Venkatesh, K., Patra, A. K., & Reinisch, B. W. (2020). F3 layer characteristics revealed by the Jicamarca incoherent scatter radar: First results. Journal of Geophysical Research: Space Physics, 125(8). https://doi.org/10.1029/2020ja028082
- Zain, A. F. M., Abdullah, S., Homam, M. J., Seman, F. C., Abdullah, M., & Ho, Y. H. (2008). Observations of the F3 layer at equatorial region during 2005. *Journal of Atmospheric and Solar-Terrestrial Physics*, 70, 918–925. https://doi.org/10.1016/j.jastp.2007.12.002
- Zhao, B., Wan, W., Reinisch, B., Yue, X., Le, H., Liu, J., & Xiong, B. (2011). Features of the F3 layer in the low-latitude ionosphere at sunset. Journal of Geophysical Research, 116, A01313. https://doi.org/10.1029/2010JA016111
- Zhao, B., Wan, W., Yue, X., Liu, L., Ren, Z., He, M., & Liu, J. (2011). Global characteristics of occurrence of an additional layer in the ionosphere observed by COSMIC/FORMOSAT-3. Geophysical Research Letters, 38, L02101. https://doi.org/10.1029/2010GL045744
- Zhao, B., Zhu, J., Xiong, B., Yue, X., Zhang, M., Wang, M., & Wan, W. (2014). An empirical model of the occurrence of an additional layer in the ionosphere from the occultation technique: Preliminary results. *Journal of Geophysical Research: Space Physics*, 119, 10204–10218. https://doi.org/10.1002/2014JA020220
- Zhou, Q. H., & Sulzer, M. P. (1997). Incoherent scatter radar observations of the F-region ionosphere at Arecibo during January 1993. *Journal of Atmospheric and Solar-Terrestrial Physics*, 59, 2213–2229. https://doi.org/10.1016/s1364-6826(97)00040-0
- Zhou, Q. H., Tepley, C. A., & Sulzer, M. P. (1995). Meteor observation by the Arecibo 430 MHz ISR I. results from time-integrated observations. Journal of Atmospheric and Solar-Terrestrial Physics, 57, 421–431. https://doi.org/10.1016/0021-9169(94)e0011-b

GONG ET AL. 8 of 8